

MASIF: Meta-learned Algorithm Selection using Implicit Fidelity Information

Anonymous authors
Paper under double-blind review

Abstract

Selecting a well-performing algorithm for a given task or dataset can be time-consuming and tedious, but is crucial for the successful day-to-day business of developing new AI & ML applications. Algorithm Selection (AS) mitigates this through a meta-model leveraging meta-information about previous tasks. However, most of the available AS methods are error-prone because they characterize a task by either cheap-to-compute properties of the dataset or evaluations of cheap proxy algorithms, called landmarks. In this work, we extend the classical AS data setup to include multi-fidelity information and empirically demonstrate how meta-learning on algorithms' learning behaviour allows us to exploit cheap test-time evidence effectively and combat myopia significantly. We further postulate a budget-regret trade-off w.r.t. the selection process. Our new selector MASIF is able to jointly interpret online evidence on a task in form of varying-length learning curves without any parametric assumption by leveraging a transformer-based encoder. This opens up new possibilities for guided rapid prototyping in data science on cheaply observed partial learning curves.

1 Introduction

Data scientists typically spend most of their time with data engineering and thus often have less time for choosing a well-performing algorithm for a given task (Anaconda, 2020). This selection process is typically powered by both the experience of the data scientist w.r.t. the performance of algorithms on previous tasks as well as a limited number of partial evaluations of the candidate algorithms on the task at hand. In doing so, a data scientist inherently carefully trades off (i) time invested into actively gathering performance information on the new task to make an informed decision and (ii) the regret in terms of performance incurred by possibly not selecting the best algorithm.

On one extreme end of this trade-off lie classical AS (Rice, 1976; Kerschke et al., 2019) approaches which characterize a task using handcrafted meta-features (Vanschoren, 2018) of the corresponding dataset. These features are supposedly informative w.r.t. the performance of an algorithm on that particular dataset **and used to learn which candidate to recommend for a new task**. In practice, such dataset meta-features may show limited association with the performance of the considered classes of algorithms (Pfahringer et al., 2000; J. Fürnkranz, 2001). In particular, so-called dataset meta-features, corresponding to cheaply-computable properties of the dataset (including simple, statistical, information-theoretic, complexity- and model-based properties (Vanschoren, 2018)), are known to be only indicative of algorithm performance to a limited degree (Pfahringer et al., 2000). Similarly, the correlation of landmarking meta-features, i.e., performances of cheap proxy algorithms computed on the new dataset, can be limited, as they hinge on how well the proxy algorithms' performances are associated with those of the pool of candidates. For instance, the performance of a decision stump might not be informative on how well a deep neural network will perform.

On the other extreme end of this trade-off lie existing learning curve approaches (Mohr & van Rijn, 2022), which exclusively invest time into gathering **premature performance approximations on the candidates and seek to extrapolate off of it**. **Examples of these approximations are validation performances of models trained for a limited amount of epochs or only on parts of the training data**. As such, learning curve approaches invest comparatively more budget on obtaining information naturally associated with the final performance

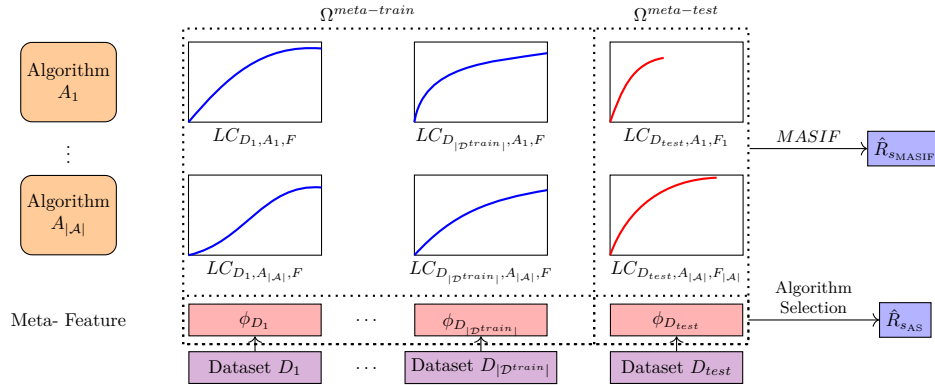


Figure 1: In contrast to classical algorithm selection trained only on meta-features, MASIF utilizes the information from both meta-features and learning curve values to predict the best performing algorithms.

39 of the classes of algorithms. A common downside to these approaches lies in their extrapolation strategy.
 40 Observing only premature approximations of the performance data with little or no meta-knowledge about an
 41 algorithm's learning behavior, learning curve methods often resort to strong parametric assumptions (Mohr &
 42 van Rijn, 2022) and are myopic in the sense that an extrapolated estimate of the final performance can only
 43 be based on the observed premature performance values. Further, with few exceptions, such as (van Rijn
 44 et al., 2015; Klein et al., 2017b; Baker et al., 2018; Long et al., 2020), they only extrapolate each algorithm
 45 independently, ignorant of possible existing relations in learning behaviors to other algorithms.

46 In this work, we propose MASIF (Meta-learned Algorithm Selection using Implicit Fidelity)¹, an approach
 47 designed to support data scientists in the AS process in a much more intuitive manner. It supports a data
 48 scientist's active discovery process on a new dataset, as it allows refining the expectation on the final ranking
 49 over algorithms based on [their](#) incremental budget allocation. This provides the user with full flexibility in
 50 different trade-offs between invested budgets and regret of the final ranking. It is however also a limitation in
 51 the sense that a user has to make this decision. As alleviation, we later provide an exemplary solution [to this](#)
 52 but note that [it](#) opens up a new area for research.

53 MASIF is powered by a transformer-based model accounting for the sequential nature of learning curves and
 54 interpreting their (partial) informational content. It learns to interpret them based on the meta-knowledge
 55 w.r.t. the candidates' learning behavior obtained from observing them on other datasets. Using this encoder
 56 and the available meta-knowledge, our model neither requires explicitly extrapolating the curves nor does
 57 it necessitate assumptions on their parametric shapes. Learning a latent representation of each curve
 58 respectively, a subsequent transformer and MLP merge the gathered test-time evidence in the form of
 59 observed premature performances. This allows learning cross-correlations between the algorithms' learning
 60 behaviors (cf. Figure 1).

61 Overall, we make the following contributions:

- 62 1. From a practical perspective, we formalize a meta-learning multi-fidelity setup that closely resembles
 63 a data scientist's workflow. Based on this we discuss the budget-regret trade-off that contemporary
 64 algorithm selectors implicitly make.
- 65 2. We introduce MASIF, a novel learning curve interpreter living in this framework, [that leverages](#)
 66 [both dataset meta-features and formulates](#) a well-informed meta-prior on the candidates' learning
 67 behaviors. It mitigates the fallacies of both, classical AS and learning curve-based approaches by
 68 interpreting multiple learning curves of varying lengths and, utilizing meta-knowledge to combat
 69 myopia², leading to a better-informed ranking with less compute on a new dataset.

¹MASIF's code is published on <https://anonymous.4open.science/status/MASIF-824D>

²We use the term **myopia** – synonym for short-sightedness to highlight the limited information horizon. In particular, these kinds of predictors/selectors can base their extrapolation only on the observed part of a curve and are ignorant w.r.t. meta-knowledge.

- 70 3. We propose a new evaluation scheme based on fidelity slices suited for demonstrating the aforementioned
71 trade-off.
- 72 4. We demonstrate the usage of our novel learning curve interpreter as an algorithm selector based on
73 a user’s budgetary and regret preferences, and evaluate its performance against other baselines on
74 several benchmarks.

75 **2 Preliminaries**

76 As we seek to unify classical AS, multi-fidelity, and learning curves, we re-examine them and offer a notation,
77 with which we later detail how selectors behave. Particularly, this notation highlights both the available
78 meta-knowledge and the associated cost of acquiring information on a new dataset.

79 **The Algorithm Selection Problem** denotes the task of finding an algorithm selector $s : \mathcal{D} \rightarrow \mathcal{A}$ from
80 the space of algorithm selectors \mathcal{S} , which selects the presumably most suitable (machine learning) algorithm
81 $A^* \in \mathcal{A}$ for a given dataset $D \in \mathcal{D}$ where \mathcal{D} is a set of datasets, also called meta-dataset. Here, suitability is
82 expressed through a costly-to-evaluate performance metric $m : \mathcal{D} \times \mathcal{A} \rightarrow \mathbb{R}$, such as accuracy or cross-entropy
83 on the test data, quantifying how well the given algorithm performs on the given dataset at the end of its
84 training process. The (hypothetical) best algorithm selector, also called the oracle, s^* , chooses the best
85 algorithm for every dataset D on the final performances:

$$s^*(D) = A^* \in \arg \max_{A \in \mathcal{A}} m(D, A) \quad (1)$$

86 **Classical Algorithm Selectors** seek to meta-learn which algorithm will perform best on a new dataset.
87 Since the performance of an algorithm $A \in \mathcal{A}$ is costly to evaluate, a complete enumeration over \mathcal{A} to select
88 the best one is often not feasible in practice, which leads to the application of machine learning to predict the
89 best algorithm. To allow learning such a selector based on meta-training data, datasets D are characterized
90 by their dataset meta-features ϕ_D and are fed as input to the selector. In the classical setting, these are
91 quickly-computable properties of a dataset, called dataset meta-features Vanschoren (2018) such as, e.g., the
92 number of data points, number of explanatory features or the entropy of a dataset’s dependent variable.

93 For the purpose of analyzing a selector’s associated cost, computing ϕ_D is part of the selector’s computational
94 budget on a meta-test dataset to gain information about it. Optionally, s can also take algorithm meta-features
95 ϕ_A as input, e.g., the number of neurons in a particular layer of a neural net (Tornede et al., 2020; Pulatov
96 et al., 2022).

97 In practice, many AS approaches, either implicitly (Xu et al., 2012; Amadini et al., 2014) or explicitly
98 (Cunha et al., 2018; Hanselle et al., 2020), compute a ranking over the algorithms \mathcal{A} and return the best one.
99 Correspondingly, as we also rely on rankings – for the remainder of this paper – we assume that a selector
100 returns a ranking from the ranking space $\mathcal{R}(\mathcal{A})$ over the discrete set \mathcal{A} , i.e., we consider algorithm selectors
101 of the form $s : \mathcal{D} \rightarrow \mathcal{R}(\mathcal{A})$.

102 In the classical setting, the data used to train a selector is called meta-training set³ to differentiate it from
103 the actual datasets D , on which the individual algorithms are trained and evaluated. It is defined as

$$\Omega^{meta-train} = \{\phi_D, \phi_A, m(D, A) | D \in \mathcal{D}^{train}, A \in \mathcal{A}\}, \quad (2)$$

104 where \mathcal{D}^{train} is a set of datasets to meta-train on. \mathcal{D}^{train} is used to train a selector s to predict rankings
105 over the known set of algorithms \mathcal{A} across datasets with minimal meta-train loss $\mathcal{L} : \mathcal{R}(\mathcal{A}) \times \mathcal{R}(\mathcal{A}) \rightarrow \mathbb{R}$. It
106 measures the error between the predicted ranking $s(D)$ and the ground-truth ranking $R_D^*(\mathcal{A}) \in \mathcal{R}(\mathcal{A})$. Hence,
107 we solve the optimization problem defined as

$$\min_{s \in \mathcal{S}} \sum_{D \in \mathcal{D}^{train}} \mathcal{L}(R_D^*(\mathcal{A}), s(D)). \quad (3)$$

³We refer to this meta-training set as meta-knowledge interchangeably.

¹⁰⁸ Similarly, the meta-test loss \mathcal{L}' of s is measured on the known set \mathcal{A} on hold-out datasets $D \in \mathcal{D}^{test}$.

$$\mathcal{L}^{test}(s) = \sum_{D \in \mathcal{D}^{test}} \mathcal{L}'(R_D^*(\mathcal{A}), s(D)). \quad (4)$$

¹⁰⁹ While \mathcal{L} usually is a differentiable training loss, during test time \mathcal{L}' does not need to have this restriction.
¹¹⁰ For the remainder, we assume this to be a regret function. In particular, since algorithm selectors return
¹¹¹ a recommendation of the most promising algorithms on the given dataset, we use the top- k regret for the
¹¹² test-loss as defined in Eq. (4)

$$\mathcal{L}_k^{test}(R_D^*(\mathcal{A}), s(D)) = \min_{A \in \text{top-}k(s(D))} m(D, A^*(D)) - m(D, A), \quad (5)$$

¹¹³ where **the top- k operator** returns the first k elements of the ranking that s recommended and $A^*(D) =$
¹¹⁴ $\arg \max_{A \in \mathcal{A}} m(D, A)$. The selector s is allowed to access the available test-time information $\{\phi_D, \phi_A | A \in \mathcal{A}\}$
¹¹⁵ for its prediction on D , resulting in the meta-test knowledge: $\Omega^{meta-test}|D = \{\phi_D, \phi_A | A \in \mathcal{A}\}$.

¹¹⁶ A particularly strong kind of meta-feature in classical AS is landmarking (Pfahringer et al., 2000). Landmarking
¹¹⁷ features report the validation performances $m(D, A)$ of cheap algorithms that are usually not in the pool of
¹¹⁸ candidates ($A \notin \mathcal{A}$) as dataset meta-features. This relaxes the assumption that meta-features need to be very
¹¹⁹ fast to compute.

¹²⁰ The utility of classical and landmarking meta-features w.r.t. the selection task depends on the alignment of
¹²¹ their description of the topology to the topology that the candidate algorithms' inductive biases are successful
¹²² on – as observed in terms of their final test performance. This is particularly true for landmarking features
¹²³ as they apply their inductive biases to the datasets' topology. Their relevance is related to the overlap in
¹²⁴ the functions that both sets of algorithms describe. For example, a shallow decision tree might be partially
¹²⁵ informative regarding the performance of other tree-based algorithms, such as random forests (Breimann,
¹²⁶ 2001) or xgboost (Chen & Guestrin, 2016). We refer to the question of information content as the *alignment*
¹²⁷ *problem* of meta-features and algorithm performance.

¹²⁸ **Multi-Fidelity Optimization** Since training a machine learning model to completion can be very expensive,
¹²⁹ multi-fidelity optimization (Li et al., 2018) aims at using cheap-to-evaluate proxies to make efficient decisions,
¹³⁰ e.g., which algorithm performs best. In automated machine learning (AutoML, Hutter et al. (2019)), these
¹³¹ proxies can include training for a limited number of epochs or training on a subset of the training data.

¹³² Formally, we seek to approximate a costly-to-evaluate function F by a **cheaper** fidelity $f_i \in \mathcal{F}$ from the space
¹³³ of fidelities \mathcal{F} . We note that also F is part of \mathcal{F} . Each fidelity f_i comes with a cost $c(x, f_i)$ to evaluate $f_i(x)$
¹³⁴ at point x . A common assumption is that the approximation quality of f_i w.r.t. F gets better in proportion
¹³⁵ to its cost $c(\cdot, f_i)$, leading to a trade-off between approximation quality and cost of the fidelity.

¹³⁶ **Learning Curves** form an ordered sub-case in multi-fidelity optimization , **that is** \mathcal{F} is cost-ordered. In
¹³⁷ our case, we consider a learning curve of an algorithm to be the performance metric $m_{lc} : \mathcal{D} \times \mathcal{A} \times \mathcal{F} \rightarrow \mathbb{R}$
¹³⁸ observed on cost-ordered fidelities f_1, \dots, F_A , where $c(x, F_A) \leq c(x, F)$ and F_A is the maximally observed
¹³⁹ fidelity for algorithm A . **Notice, that the definition of m_{lc} generalizes the former notion of m to be observable**
¹⁴⁰ **at multiple fidelities.** Formally, a learning curve can be defined as

$$LC_{D, A, F_A} = (m_{lc}(D, A, f))_{f=f_1, \dots, F_A} . \quad (6)$$

¹⁴¹ Notably, we distinguish between a partial learning curve, i.e., $F_A \neq F$, and a full learning curve, i.e., $F_A = F$.
¹⁴² Each algorithm may be observed at a different maximum fidelity F_A , since a user may decide to spend
¹⁴³ different amounts of computing resources to evaluate different algorithms A .

144 3 MASIF: Interpreting Partial Learning Curves Jointly

145 In this section, we introduce our core contributions: (i) extending the classical AS setup by adding multi-fidelity information, allowing for a more detailed analysis of the budget-regret trade-off of algorithm selectors;
 146 (ii) our transformer-based MASIF approach as an efficient method for this extended data setup; and (iii) a
 147 data augmentation scheme to achieve strong predictive performance and enable MASIF to accept arbitrary
 148 budget allocation strategies.

150 3.1 Extending Algorithm Selection by Multi-Fidelity Information

151 In addition to dataset meta-features, we propose to use information from learning curves as multi-fidelity
 152 information for AS. This provides a new source of information by prematurely inquiring about a new dataset's
 153 topology from the perspective of the candidates' inductive biases that is both relatively cheap and surely
 154 well-aligned. We summarize this setup in Figure 1.

155 **Meta-Training Data** The aforementioned idea extends our available training *meta-knowledge* in Eq. (2)
 156 and Eq. (3) by fidelity information, amounting to

$$\Omega^{meta-train} = \{\phi_D, \phi_A, LC_{D,A,F} | D \in \mathcal{D}^{train}, A \in \mathcal{A}\} \quad (7)$$

157 where the learning curves $LC_{D,A,F} \in \mathbb{R}^F$ replace the performance values $m(D, A) \in \mathbb{R}$ in Eq. (2). For our
 158 experiments, we observed full learning curves up to the maximal fidelity F for the meta-training dataset.
 159 The meta-training dataset encodes several aspects of the available meta-knowledge: (i) the relation of the
 160 algorithm's performance w.r.t. the dataset's topology, (ii) how information about the algorithm's inductive
 161 bias is unrolled across fidelities marginally, and (iii) how the learning behavior of different algorithms relate
 162 to each other on the datasets they are applied to.

163 **Meta-Testing Data** The meta-testing phase provides *partial* learning curves observed on a new hold-out
 164 dataset. The set of curves provides evidence of the dataset's topology observed through the lens of the
 165 algorithms. The available information at test time for our selector s in Eq. (4) is:

$$\Omega^{meta-test} = \{\phi_D, \phi_A, LC_{D,A,F_A} |, F_A \leq F, A \in \mathcal{A}, D \in \mathcal{D}\}. \quad (8)$$

166 Notably, depending on a user's budgetary preferences, some of the learning curves may be revealed nearly
 167 entirely or not at all; in general, we assume that the set of all learning curves may be incomplete. Since an
 168 algorithm selector returns a ranking over the algorithms on the given dataset, we use the top- k regret for the
 169 test-loss on the final fidelity F as defined in Eq. (4).

170 3.2 MASIF Architecture

171 We choose a deep learning architecture because of its functional flexibility and its non-parametric modelling.
 172 However, we have to exploit the little data typically available in AS without grossly over-fitting to the
 173 meta-data. Our proposed architecture is displayed in Figure 2 and consists of five main building blocks:

174 **Block 1: Dataset meta-feature embedding** Assuming some valuable information on the topology in
 175 the classical meta-features f_D , an MLP encodes them into a latent space. Utilizing this cheap set of features,
 176 from an informational standpoint, our method can only improve over classical AS methods and further allows
 177 us to contextualize the observed learning curves to the observed dataset. If, for instance, ϕ_D conveys some
 178 information regarding the complexity of the dataset, this may be indicative of how fast an algorithm might
 179 learn, affecting the shape of the curve.

180 **Block 2: Learning curve preprocessing** As preprocessing of the learning curves, we apply zero-padding
 181 to fill the learning curves up to the final fidelity F and accordingly generate a mask to store the padding

182 information. To avoid technical issues with fully masked sequences, we append an extra learnable End Of
 183 Sequence (EOS) token (Dosovitskiy et al., 2020). We then apply a shared MLP separately to each position
 184 of each learning curve. Embedding each position of a learning curve individually increases the expressivity
 185 of our one-dimensional learning curve sequences into e dimensions akin to BERT’s vector representations
 186 for each word (Devlin et al., 2019). To overcome the transformer’s native positional ignorance, we follow
 187 Vaswani et al. (2017) in encoding the positional information with sine and cosine functions and adding these
 188 values to the embedded learning curves. This is a crucial step in preserving the sequence information, which
 189 in our case conveys the order in learning curves.

190 **Block 3: Learning curve embedding** We use
 191 a variation of the transformer-encoder proposed by
 192 Vaswani et al. (2017) on the set of partially ob-
 193 served learning curves LC_{D,A,F_A} of each algorithm
 194 $A \in \mathcal{A}$. This translates the (incomplete/masked)
 195 learning curve sequence into a latent vector repre-
 196 sentation enriched with the meta-knowledge of the
 197 algorithms’ marginal learning behaviors.

198 Since the classical dataset meta-features may carry
 199 valuable information (if they are available) for the
 200 amount and variability of information at each position
 201 in the sequence, we introduce a mechanism we dub
 202 *guided attention*. Similar to the classical attention
 203 module, our encoder receives a query Q , key K , and
 204 value V tensor, containing the preprocessed learning
 205 curves from Block 2. We multiply the query Q of the
 206 attention heads element-wise with a linear projection
 207 of the embedding described in Block 1 if dataset meta-
 208 features are available. The projection’s role is merely
 209 to fit the shape of Q . To increase parallelism and
 210 reduce the number of learnable parameters, we use
 211 a batch trick by only processing one dataset at a
 212 time, but conceive the set of algorithms \mathcal{A} to be a
 213 batch of dimensions $[\mathcal{A}, \mathcal{F}, e]$, that is processed in
 214 parallel. The attention-guided transformer-encoder
 215 layer is repeated N times to yield a marginal summary
 216 of the latent representation of each of the learning
 217 curves. The order of the batch is held fixed over
 218 all datasets, s.t. the subsequent module receives the
 219 latent vector representation of an algorithm’s learning
 220 curve at the exact same position every time.

221 Given the generated feature maps, we reduce the
 222 $[\mathcal{A}, \mathcal{F}, e]$ -dimensional tensor along the fidelity dimen-
 223 sion, using a learnable weighted average over the fi-
 224 delities \mathcal{F} applied independently over \mathcal{A} , resulting in
 225 e -dimensional vectors. This formulates a joint rep-
 226 resentation of the evidence on D encoded in these vec-
 227 tors. Given the properties of the target dataset, the
 228 model should focus on different stages of the learning
 229 curves. Therefore, we make these weights learnable.
 230 More precisely, if dataset meta-features are available,
 231 the dataset meta-feature embedding to the size of \mathcal{F} . Otherwise, these weights directly become learnable
 232 parameters.

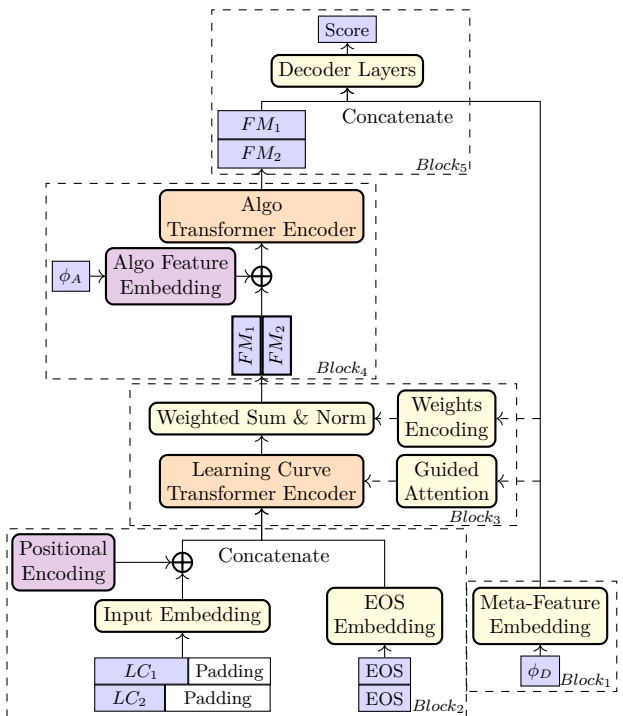


Figure 2: MASIF Architecture. Blue rectangles represent data, yellow rectangles denote MLP layers, purple rectangles indicate positional encodings, and orange rectangles are transformer layers. MASIF receives the partial learning curves of all the algorithms $LC_{D,A,F_A} \forall A \in \mathcal{A}$ (in this figure, we only show two learning curves, i.e., LC_1 and LC_2 , indicating $LC_{D,A_1,F_{A_1}}$ and $LC_{D,A_2,F_{A_2}}$). The two transformer encoder layers apply attention operations on the fidelity and the algorithm dimensions, respectively. Therefore, the output of each transformer needs to be transposed to fit the dimension. The output of the last transformer (FM_1 and FM_2) is concatenated with the embedded meta-features ϕ_D . Finally, the joint features are fed to the decoder to get the predicted ranks.

233 **Block 4: Fusing the evidence.** The model up until this point is still unaware of the cross-algorithm
 234 information between different learning curves, which is essential to predict the relative ranking of each
 235 algorithm. Therefore, we build another transformer on top of the first transformer that fuses the evidence on
 236 the topology derived from the partial learning curves of all $A \in \mathcal{A}$. The rationale is that since the algorithms
 237 are always presented in the same position, the position of these vectors holds meaning. From the perspective
 238 of BERT, each algorithm vector is the embedding to a token, and the sequence of algorithms is a sentence.
 239 Therefore, we transpose the set of representations and make the batch dimension explicit $[1, A, e]$. To let the
 240 transformer identify different algorithms, we encode the algorithms' features (i.e., their hyperparameters or a
 241 simple one-hot encoding when no hyperparameter is available) as positional encoding and attach them to the
 242 generated transformations. **The rationale for treating the algorithm meta-feature embedding as a positional
 243 encoding – if corresponding features are available – is to give the learning curve embeddings more context at
 244 best and provide an alternative index that replaces the one-hot encoding at worst.** Treating these algorithm
 245 representations as positional encodings should aid the second transformer encoder in how to fuse the sources
 246 of information. We have added an ablation on this design choice in Appendix 8.

247 **Block 5: Ranking** Yet again, we employ an MLP on the concatenation of the vectorized evidence and the
 248 dataset meta-feature embedding to fuse their information and project to the size $n_{\mathcal{A}} = |\mathcal{A}|$. The returned
 249 values are scores for the respective algorithms, corresponding to latent utility values, which are used to
 250 construct a ranking across the algorithms. As an objective, we would like to maximize the Spearman rank
 251 correlation between predicted and true algorithm ranks. In order to obtain a differentiable loss, we thus
 252 leverage a differentiable sorting algorithm (Blondel et al., 2020) to compute the training loss.

253 3.3 Data Augmentation

254 Since AS usually only has a limited amount of dataset-algorithm combinations in its meta-training dataset for
 255 which we observe a single learning curve instantiation, respectively, we use a data augmentation strategy. **We
 256 mask the learning curves by** sampling the available learning curve length F_A uniformly and independently from
 257 $[0, F]$, where 0 indicates a complete lack of information on that learning curve. **In addition to circumventing
 258 meta-overfitting,** this strategy allows our model to be presented with any budget allocation (combination of
 259 fidelities), i.e. $\{F_A \in \mathcal{F} \cup \{0\}\}_{A \in \mathcal{A}}$ – including the option of not evaluating a curve during test-time.

260 3.4 Hyperparameters

261 To foster reproducibility, we list the following hyperparameter choices in the above architecture. Details
 262 regarding their choices, including ablations, can be found in Appendix A.4. We encode all the meta-features
 263 (i.e., ϕ_D and ϕ_A) with a 2-layer MLP (with hidden size of 128 and 64) into an embedding of size 64. All
 264 transformer encoder layers in MASIF have the same architecture with hidden size 128 and 4 attention heads.
 265 Each of the transformer encoders (Learning Curve Transformer Encoder and Algo Transformer Encoder)
 266 have 2 transformer layers applied with a dropout rate of 0.2. We train MASIF with an ADAM optimizer
 267 with a learning rate of 0.001 and beta values as 0.9 and 0.999 for 500 epochs while neither learning rate
 268 scheduler nor weight decay are employed.

269 3.5 MASIF's Benefits

270 The transformer encoding of the learning curves offers significant advantages: at no point do the learning
 271 curves require extrapolation. Instead, only their informational content is summarized and transformed into
 272 a conditioned ranking score. Our method, therefore, does not fall victim to error propagation as often
 273 encountered in time series regression or multi-label classification (Senge et al., 2012). Additionally, leveraging
 274 the meta-knowledge **obtained by observing** the learning curves of the same algorithms on meta-training
 275 datasets, we combat multi-fidelity's inherent myopia problem effectively and can be fully non-parametric in
 276 the shape of the learning curves due to a strong meta-prior encoded in the weights of our architecture. To this
 277 end, MASIF exploits **the available meta-knowledge extensively of having** observed the algorithms' learning
 278 curves on multiple datasets jointly. Depending on the type of algorithms and fidelity, this meta-knowledge in
 279 the form of algorithms' learning curves comes at almost no cost when collecting the meta-training data in the

280 classical AS setting. Crucially, taking a multi-fidelity lens – independent of whether or not we include classical
 281 and landmarking meta-features – its ranking ability is no longer bounded by the alignment of tediously
 282 handcrafted and highly task-specific meta-features. Instead, it is now governed by the trade-off between
 283 the approximation quality of the fidelities and the induced cost of querying them. It does, however, readily
 284 consider expert knowledge in form of dataset meta-features to contextualize the observed learning curves.

285 Given some budget allocation, the MASIF model corresponds to an algorithm selector since it produces
 286 a ranking that takes all the available meta-knowledge and the gathered evidence on the test dataset into
 287 account. However, since any budget allocation is possible, it can be readily utilized not only as a selector but
 288 as an interpreter of the incrementally arriving performance feedback from the budget allocation. Queried
 289 continuously as more evidence arrives, users can observe the shift in expectation on the final ranking,
 290 conditioned on what has been observed so far. This application mode makes this model an actionable support
 291 system for data science practitioners facing the AS problem.

292 The trade-off between approximation quality and budget costs opens up the opportunity of defining schedulers
 293 that successively queries the fidelities of algorithms (i.e., extending their learning curves) by exploiting our
 294 model. Since our contribution focuses on the model part and since MASIF’s model works with arbitrary
 295 strategies for deciding the budget allocation, in our experiments we show exemplary results with the
 296 prominent scheduling approach of *Successive Halving (SH)* (Jamieson & Talwalkar, 2016). While the original
 297 SH procedure in each “bracket” retains the current top-performing algorithms, our variant, dubbed SH
 298 Scheduler retains those that based on the current observation MASIF predicts to be top-performing on the
 299 final ranking.

300 4 Experiments

301 In this section, we first introduce a new evaluation protocol for our proposed extension of the classical AS
 302 meta-data setup with added fidelity information. Then, we detail our baselines along with their perks and
 303 shortcomings, briefly describe the meta-datasets we use as benchmarks and subsequently detail our findings.

304 4.1 Fidelity-Slice Evaluation Protocol

305 In order to assess the ability of methods to improve performance as a function of the length of the observed
 306 learning curves, we introduce a standardized *fidelity-slice evaluation protocol* that demonstrates how a
 307 method’s top- k regret w.r.t. the true ranking changes as more and more fidelity information becomes available.
 308 This way, we can observe the progression of an information-bounded expectation traded with the additional
 309 cost incurred. In particular, this protocol computes the regret of $s(D)$ ’s prediction on the test set at a
 310 gradually increasing amount of available fidelity slices; i.e. all algorithms are observed up to the same fidelity.

311 4.2 Baselines

312 We consider several baselines to highlight different aspects of our setup and architecture ranging from simple
 313 random rankings over classical AS to an extended version of successive halving.

314 **Random Baseline.** Consider a selector that randomly guesses the ranking. It will lead to a regret
 315 distribution depending on (i) k in top- k (ii) the spread and clustering of learning curves on a single dataset,
 316 indicating the hardness of the ranking task and (iii) the performance scale. This baseline averages the
 317 obtainable regret of each dataset instance. It contextualizes the selectors’ regrets across tasks.

318 **Classical Algorithm Selection.** While AS allows for generalization over dataset instances, its limitation
 319 in ranking performance lies in the limited expressivity and relevance of the employed meta-features. Therefore,
 320 we seek to demonstrate the benefit of partial learning curves as an addition to classical meta-features. For
 321 that purpose, we compare against SATzilla’11 (Xu et al., 2012), a portfolio-based algorithm selector, which
 322 models the AS problem as a multi-class classification problem and solves it using a cost-sensitive all-pairs
 323 decomposition to single label classification by employing one random forest classifier for each subproblem.

324 The final ranking is then obtained by voting. This selector is irrespective of fidelity and will produce a
 325 constant value in the slice evaluation protocol.

326 **Fidelity enabled Algorithm Selection.** Classical AS only considers the dataset and algorithms' meta-
 327 features. Considering that our method's learning curve embedding could be conceived to be a latent
 328 meta-feature ϕ_D , classical AS can conceptually similarly be enabled. To achieve that, the classical ϕ_D can be
 329 extended by $m(D, A, f)$ for some intermediate fidelities $f < F$ observed for all $A \in \mathcal{A}$. Given $f \in \mathcal{F}'$ with
 330 $\mathcal{F}' \subset \mathcal{F}$, this implies that $|\mathcal{A}| \cdot |\mathcal{F}'|$ columns are added to the feature space. Consequently, we limit $|\mathcal{F}'|$ to a
 331 subset of evenly spaced fidelities.⁴ In the slice evaluation protocol, the intermediate fidelities are added only
 332 up until the horizon of the protocol.

333 **Parametric Learning Curve Predictors.** Neglecting any meta-knowledge and combating myopia through
 334 strong parametric assumptions, a naive learning curve predictor can interpret any partial information available.
 335 Such a predictor fits a parametric curve to each partial curve and extrapolates it to the final performance. The
 336 selector s independently extrapolates to the final performances and ranks the algorithms according to these.
 337 To create a meaningful and more expressive selector that mimics a practitioner's attempt at extrapolating
 338 learning curves for AS, we fit all parametric curves described in Mohr et al. (2022) and select the best fitting
 339 one on the observed part for extrapolation. This baseline highlights that learning curve predictors are used
 340 as algorithm selectors by practitioners when lacking meta-knowledge. Surpassing this baseline indicates that
 341 our method's expectation of the ranking can benefit from joined meta-knowledge about an algorithm's past
 342 progressions and related learning behaviors.

343

344 **LCNet.** Learning curve prediction with Bayesian neural networks Klein et al. (2017b), originally designed
 345 for hyperparameter optimization problems can be applied to our algorithm selection task whenever hyperpa-
 346 rameters or algorithm meta-features are available on a benchmark. The underlying Bayesian Neural Network
 347 takes the hyperparameter configuration and the fidelity level at which it is observed as input and outputs
 348 both a variance and a mean prediction. The mean is built of a weighted ensemble of the parametrizations for
 349 a fixed set of parametric learning curves. It is a meta-agnostic but expressive parametric baseline.

350 **IMFAS.** Implicit Multi-Fidelity Algorithm Selection (IMFAS) (Mohan et al., 2022) utilizes an LSTM-
 351 based architecture that initializes its hidden state using an MLP encoding of the dataset meta-features and
 352 auto-regressively accepts slices of fidelity to refine the expectation of the ranking.

353 **Successive Halving (SH).** Despite its simplicity, SH (Karnin et al., 2013; Jamieson & Talwalkar, 2016)
 354 has several desirable properties to compare against in terms of its interpretation of partial learning curves. It
 355 is a meta-agnostic and therefore myopic, fidelity-aware but non-parametric method. SH naturally produces
 356 a myopic ranking, by the level at which it terminates the algorithm. Ties within this set of terminated
 357 algorithms are resolved by their relative performances on that bracket. Limiting the fidelity information
 358 horizon of the selectors implies that for every such horizon, we need to recompute the ranking induced by
 359 SH. Notably, to permit SH the same information horizon, the last available fidelity in its schedule will be
 360 the maximum fidelity in that horizon. The benefit of this convention is that SH has access to the same
 361 fidelity information and can make better decisions for the algorithms it recommends. Its drawback of SH as a
 362 baseline is that the incurred cost differs from that of our method.

363 4.3 Datasets

364 Where possible, we utilize training, validation, and test learning curves for the training of all approaches.
 365 These are obtained by splitting each dataset in the corresponding benchmark in training, validation, and test
 366 data, training the corresponding algorithms on the training data under each fidelity, and computing their
 367 validation and test performance corresponding to the model trained for that fidelity. While the classical AS
 368 approaches only receive the final test performance on the meta-train datasets as training data, we provide

⁴In our experiment, this amounts to the fidelity sequence [0, 0.2, 0.4, 0.6, 0.8, 1].

(partial) validation curves to SH, the learning curve approaches, and MASIF to train on, but measure the final regret with respect to the full fidelity test performance. The same applies when the approaches are applied to new test datasets. We then assess the performance of each approach by performing a 10-fold outer cross-validation of the meta-dataset. We use three different benchmarks (more details in Appendix A.1):

- **Synthetic.** We constructed the Synthetic meta-dataset based on parametric learning curves taken from Mohr et al. (2022), specifically to demonstrate the myopia of SH and learning curve predictors. Particularly, it introduces noisy curves, that exhibit crossing points. We show how MASIF alleviates myopia through strong prior knowledge w.r.t. the functional family an algorithm is adhering to.
- **Task-set.** Task-set (Metz et al., 2020) is a fairly noisy real-world dataset based on parameterizations of the Adam optimizer (Kingma & Ba, 2015), with a variety of learning rates, run on a large variety of modern deep learning architectures and datasets.
- **Scikit-CC18.** With Scikit-CC18, we evaluated multiple well-known scikit-learn (Pedregosa et al., 2011) algorithms on the classification benchmark OpenML-CC18 (Bischl et al., 2021b).
- **LCBench.** LCBench (Zimmer et al., 2021) is a learning curve benchmark of different funnel-shaped neural networks and hyperparameters for tabular data. We sub-sampled the set of configurations to only include 170 combinations as algorithms to be selected.

These four benchmarks differ in their availability of dataset and algorithm meta-features: while Synthetic and Task-set exhibit neither, Scikit-CC18 and LCBench exhibits both. Since Scikit-CC18 and LCBench are the only benchmarks with available dataset meta-features ϕ_D , we can only evaluate SATzilla and IMFAS on them. Similarly, the dataset and algorithm meta-features can only be exploited by our architecture on these benchmarks.

4.4 Results

Summarizing our results, depicted in Figure 3, on benchmarks Task-set and Synthetic, MASIF outperforms the other methods in terms of top-1 regret, and on Scikit-CC18 it performs competitively. Additional results on an NLP subset of Task-set can be found in Appendix A.2, as they show the overall same tendencies. Since our baselines applied in the slice-evaluation protocol on their own already reveal a few features of the meta-datasets we would like to detail their implications first. Afterwards, we discuss our experiments in light of the available meta-knowledge w.r.t. myopia and parametric assumptions.

Benchmark Difficulty. First of all, paying close attention to the random baseline and SH already indicates the difficulty of a benchmark; the random baseline can be thought of as an upper regret bound for any meaningful selector. If this threshold already incurs a small regret as in Scikit-CC18, this implies that there is only little to gain, increasing the difficulty for a selector to improve. SH, on the other hand, pays close attention to the earlier parts of the curve. If this is already very indicative in terms of the final performance, only few crossings of the curves occur and thus decisions based on low-fidelity are good w.r.t. final performance. In this sense, Scikit-CC18 is an arguably easier meta-dataset than Task-set, as SH is close to oracle performance after a few fidelity slices in their top-3 regrets (compare with Figure A.3). SH’s detrimental performance on Task-set on the other hand likely is due to the high variability and crossing of the curves, indicating the difficulty of this meta-dataset. The fact that no method obtains zero regret on Task-set at the final fidelity originates from the noisy target as indicated by the final fidelity of the parametric baseline. Moreover, parametric learning curve is (almost) guaranteed to yield oracle performance on Synthetic by construction. Inspired by Multi-LCNet (Jawed et al., 2021), which uses LCBench as its sole benchmark, we ran our experiments on LCBench as well. However, we find that LCBench is not a strong benchmark for our setup, due to (i) the confidence bounds overlap (ii) the very small regret of around 0.02 of most approaches and (iii) the fact that all of the meta-aware selectors do not require additional fidelity information to adjust their prior. This is additionally supported by (i) SH’s strong low-fidelity performance with only little gain by fidelity and (ii) both SH’s and the parametric learning curve baseline’s strong final performances.

The Role of Meta-knowledge. We highlight the fact that zero-fidelity corresponds to the classical AS setup and expresses the prior belief of a selector in the final performance based on the meta-knowledge. Baring

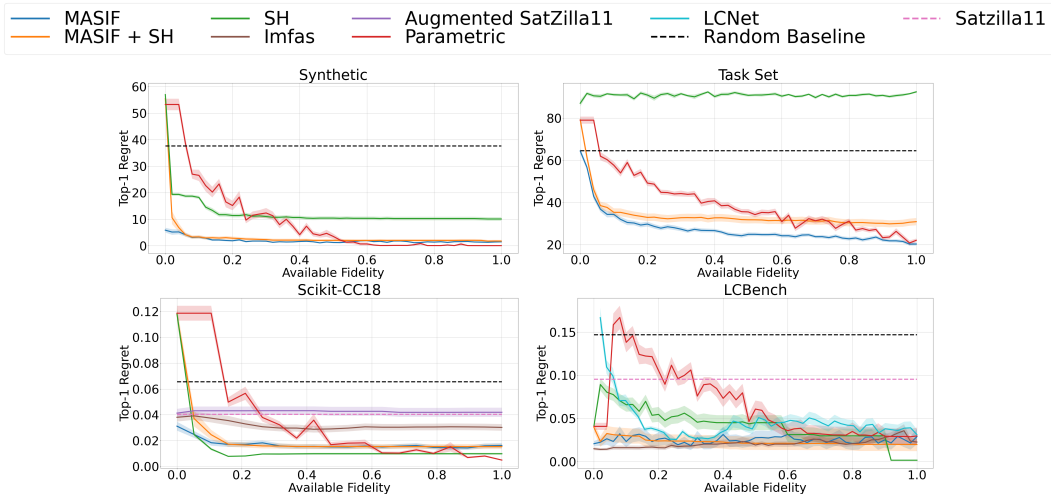


Figure 3: Average test-set top-1 regret over ten meta-dataset folds in the slice evaluation protocol. Available fidelity is expressed in the share of the target fidelity’s budget. The standard error bands originate from five repetitions for each of the ten folds. **Note:** Scikit-CC18 and LCBench exhibit dataset meta-features, while Synthetic and Task-set do not. Task-set is reported for the image data subset.

417 this in mind, the fact that MASIF is almost constant and already top-performing on Synthetic indicates that
 418 the strong prior derived from meta-knowledge is already sufficient – which in the case of Synthetic is by
 419 construction. A decrease in regret indicates that the [by adding](#) additional test-time fidelity information up to
 420 F_{max} refines this meta-knowledge-based belief.

421 The trajectory of the parametric learning curves is a strong myopic baseline to demonstrate the effect of
 422 meta-knowledge, as more fidelity becomes available. SH similarly acts as a myopic baseline, but its schedule’s
 423 path dependency may deny it to recover from early mistakes and hence result in sub-optimal states even when
 424 full fidelity is available. The steep decay in regret of MASIF at the beginning of its regret curves on Task-set
 425 and the minor adjustments on Scikit-CC18 demonstrate [the desirable property](#), that MASIF’s prior can
 426 indeed be improved based on incoming fidelity information. Similarly, IMFAS (Mohan et al., 2022) exhibits,
 427 albeit far less pronounced, such a decay indicating that fidelity information also helps it. Its dependence
 428 on classical dataset meta-features as initialization and its autoregressive nature prevent it from excelling at
 429 increasingly revealed fidelity information [and likely even is the cause of its slight deterioration on LCBench](#).
 430 Its strong dependence on classical dataset meta-features also prevents it from being runnable on Synthetic
 431 and Task-set.

432 A direct comparison of MASIF with the parametric learning curve baseline on Synthetic and Task-set in
 433 terms of reduced variability and consistent superiority – already – in the early stages highlights the benefit
 434 of having meta-learned the algorithms’ learning behavior to combat myopia effectively. The SH Scheduler
 435 observed on Task-set supports this fact. When comparing SH against SH Scheduler on this noisy dataset it is
 436 apparent, that the gained meta-knowledge becomes the main driver of the regret curve. Notably, the SH
 437 Scheduler’s curve appears inferior at first to MASIF’s trajectory, until we factor in that MASIF follows the
 438 slice evaluation protocol very closely and the SH Scheduler has considerably less overall budget available
 439 due to the SH’s budget allocation strategy. It also suffers from its path dependency, yielding slightly inferior
 440 results to MASIF, but at considerably less cost. This regret gap diminishes with lower benchmark difficulty
 441 in terms of accuracy of the meta-knowledge, as can be observed on Synthetic and Scikit-CC18, when strong
 442 prior beliefs facilitate making good decisions early on. This most prominently demonstrates the budget-regret
 443 trade-off a scheduler incurs. A comparison of SATzilla11 and our variants on Scikit-CC18 similarly highlights
 444 this trade-off; SATzilla11 incurs zero additional cost at test time over the computation of dataset meta-features
 445 which are available to all three. Its prediction must fully rely on its prior, but MASIF can reduce SATzilla11’s
 446 regret at a small additional cost during test time, having learned the algorithms’ learning behaviors.

447 To our surprise, fidelity-enabled SATzilla11 performs similarly to that without fidelity information on Scikit-
 448 CC18. This fidelity-aware but non-parametric baseline ignores the naturally occurring sequential nature and
 449 fails to improve over its fidelity-agnostic variant. It remains unclear as to why this occurs in our experiments,
 450 **but we** conjecture that it grossly overfits the meta-training data due to its sizable feature space.

451 As the ablation results in Appendix A.4 suggest, the usefulness of the raw dataset & algorithm meta-features
 452 in the two datasets is negligible at best. This has two implications: first, the meta-learned multi-fidelity
 453 information is the definite driver of our model and well outperforms the classical meta-feature-based approaches.
 454 A small caveat to the results of classical methods is their handcrafted nature. Considerable time investment
 455 into the generation and preprocessing of task-specific meta-features may yield improved regret performances
 456 for all models accepting dataset meta-features. This is why, despite the lack of strong evidence for its
 457 improvement, we keep the dataset- and algorithm meta-features as an optional part of our architecture.

458 5 Related Work

459 Classical AS approaches are based on the assumption that dataset instances (tasks) can be represented using
 460 meta-features. They learn mappings between datasets and algorithms w.r.t. performance based on such
 461 pre-computed meta-features. Most methods to learn such mappings in the literature either leverage regression
 462 techniques (Xu et al., 2008; Bischl et al., 2016), ranking techniques (Cunha et al., 2018; Abdulrahman et al.,
 463 2018), collaborative filtering (Stern et al., 2010; Fusi et al., 2018), instance-based learning approaches (Amadini
 464 et al., 2014; Kadioglu et al., 2010) or mixtures of the aforementioned techniques (Hanselle et al., 2020; Fehring
 465 et al., 2022). All of these approaches, however, suffer from the same limitation: Pre-computed meta-features,
 466 as mentioned earlier, can **be in** sufficient **in** characterizing the datasets and algorithms due to the alignment
 467 problem discussed in Section 2. Our approach circumvents the alignment issue by landmarking datasets
 468 directly based on the candidate algorithms' inductive biases, as unrolled in their partial learning curves, and
 469 predicts a rank over the set of candidate algorithms.

470 The idea of exploiting partial learning curves has previously been explored in some works. SAM (Leite &
 471 Brazdil, 2004) non-parametrically matched partial learning curves to the closest in terms of shape from the
 472 observed meta-learning curves using kNN, while van Rijn et al. (2015) reduced the cost of cross-validation by
 473 exploiting the similarity of the partially-observed rankings with those of the meta-datasets and using the most
 474 similar learning curve as surrogates. Mohr & van Rijn (2021) extended this approach by terminating less
 475 promising candidates early on based on their predicted learning curves modelled in a semi-parametric way
 476 under the assumption of concavity. In contrast to this explicit prediction of the missing parts of the learning
 477 curves, MASIF *implicitly* meta-learns correlations between the partial performances of algorithms to predict
 478 a ranking. Leite & Brazdil (2010) pursue a cheaper and meta-informed alternative to cross-validation that
 479 evaluates the collection of fidelities using SAM, and then actively schedules them in a cost-aware manner.

480 **Similarly, multi-fidelity optimization can be used in hyperparameter optimization** (Bischl et al., 2021a) **to**
 481 **save computing resources.** It allows the optimizer to actively query new candidate configurations, unlike the
 482 classical AS setup. Corresponding methods can be categorized into bandit-based ones (e.g. SH (Jamieson &
 483 Talwalkar, 2016), ASHA (Li et al., 2020), PASHA (Bohdal et al., 2022), HB (Li et al., 2018), DEHB (Awad
 484 et al., 2021), BOHB (Falkner et al., 2018), ID-HB (Brandt et al., 2023), SMAC3 (Lindauer et al., 2022),
 485 DSMAC (Sui & Yu, 2020), BOCA (Kandasamy et al., 2017)), cost-aware ones (e.g. BOIL (Nguyen et al.,
 486 2020), FaBOLAS (Klein et al., 2017a)), and learning curve extrapolating ones (e.g. Freeze-Thaw (Swersky
 487 et al., 2014), Speeding up Automatic Hyperparameter Optimization of Deep Neural Networks (Domhan
 488 et al., 2015), DyHPO (Wistuba et al., 2022), LCNet (Klein et al., 2017c), as well as Multi-LCNet (Jawed
 489 et al., 2021)).

490 **As Multi-LCNet is the one closest related to ours in terms of its setting on the hyperparameter optimization**
 491 **side, it is worth investigating the differences more closely.** While they use a related $\Omega^{meta-train}$ and $\Omega^{meta-test}$
 492 data setup, the work has substantial differences and rigid assumptions, which make us abstain from an
 493 experimental comparison of MASIF to it, as a fair comparison is not possible. The core differences are
 494 threefold; 1. they consider a hyperparameter optimization multi-fidelity problem 2. their model can assume
 495 the existence of auxiliary curves for a single algorithm, because of the narrow definition of an algorithm and

496 3. they use this multi-modal data in an autoregressive way for the explicit extrapolation of a single curve at a
 497 time. A more detailed discussion is deferred to Appendix A.5.

498 In summary, all of these methods are applications of multi-fidelity in hyperparameter optimization. From the
 499 lens of our setup, they are applied to a relaxation of the hyperparameter search space that is out of scope here.⁵
 500 Crucially the first two kinds of methods primarily focus on the problem of scheduling the configuration and
 501 endowing it with a budget. On the other hand, the last kind of method focuses on marginally extrapolating
 502 learning curves for a single configuration irrespective of previously seen learning curves on the same dataset.
 503 MASIF differs from these approaches in that it focuses on jointly interpreting the learning curves in the AS
 504 setup and does not imply any schedule.

505 Two approaches orthogonal to ours, although bearing some resemblances in terms of setup, are Meta-REVEAL
 506 (Nguyen et al., 2021) and MetaBu (Rakotoarison et al., 2021). Meta-REVEAL focuses on scheduling the
 507 algorithms and fidelities through a Reinforcement Learning perspective by modelling it as a REVEAL game.
 508 The agent acts on a discrete action space that does not account for the correlations between learning curves.
 509 As we do not focus on schedule but on learning cross-correlations on the learning behavior, we refrain from a
 510 comparison. Consequently, using the estimates produced by MASIF can provide a pre-processed action space
 511 for their problem. MetaBu extends the classical AS idea by relating dataset meta-features and algorithms'
 512 hyperparameters using a learned optimal transport map. They, however, ignore that the dataset meta-features
 513 cannot sufficiently characterize the dataset, thus, subsequently falling victim to the same fallacies as the
 514 methods mentioned before.

515 6 Conclusion

516 In this work, we revisited classical meta-learning- and learning curve-based approaches to AS from the
 517 perspective of a trade-off between the budget they invest in inquiring information about a new dataset and the
 518 corresponding regret of choosing an inferior algorithm. Doing so, we argued that both of these selector classes
 519 are on opposite ends of the spectrum in this trade-off and both suffer from severe limitations, likely leaving
 520 data scientists with a selected algorithm [that is inferior](#). To alleviate this, we present MASIF, an algorithm
 521 selector designed to support data scientists in the selection process in a far more native manner. Its position
 522 in the spectrum can be controlled by the data scientist depending on their budgetary constraints. MASIF
 523 leverages a transformer-encoder-based architecture to model the performance of algorithms across both,
 524 fidelities and algorithms in the form of learning curves of varying lengths. As such, it alleviates the myopia
 525 of many existing learning curve-based approaches while making no parametric assumptions on the learning
 526 curves it can model. Crucially, our selector utilizes computation from previous selections as meta-knowledge.
 527 In an extensive experimental study on four different benchmarks, we showed that MASIF outperforms existing
 528 meta-learning-based approaches in terms of the regret of the selected algorithm and learning curve-based
 529 algorithm selectors in terms of regret for the invested budget. As such, MASIF is not only an AS approach
 530 designed to support the data scientist in practice by leaving the concrete instantiation of the trade-off to
 531 their preference but also yields state-of-the-art AS performance.

532 7 Future Work

533 The aforementioned budget-regret trade-off leads to a multi-objective view of the AS problem, where both
 534 the budget invested and the regret of the corresponding algorithm selector are rivalling objectives. This
 535 holistic view naturally suggests tackling the problem with multi-objective methods to be able to present a
 536 Pareto front of selectors to choose from, suited to a data scientist's budget-regret preferences in the face
 537 of uncertainty. This line of work is orthogonal to previous multi-objective work in Algorithm Selection
 538 (Bossek & Trautmann, 2018). Any instance on this Pareto front is a scheduler of sorts. Determining how a
 539 scheduler knowledgeable in learning behaviors should choose its budget allocation sequentially and in the
 540 face of uncertainty inspires research on its own. Lastly, in the current form of this work, the algorithms are
 541 predominantly represented through their learning curves and we use algorithm meta-features in a relatively
 542 limited manner. Multi-LCNet (Jawed et al., 2021) presumes that using hyperparameters among other

⁵SH-based methods are living on a discretized version of this broader space.

informative algorithm meta-features may also be beneficial in contextualizing a learning curve. In that sense, a natural extension to the scope of this work is the transition from tackling the AS problem to tackling the hyperparameter optimization problem. In contrast to existing approaches, we will seek to extract the joint topology evidence derived from the observed partial learning curves in order to tackle this problem.

References

- S. Abdulrahman, P. Brazdil, J. van Rijn, and J. Vanschoren. Speeding up algorithm selection using average ranking and active testing by introducing runtime. *Machine Learning*, 107(1):79–108, 2018.
- R. Amadini, M. Gabbrielli, and J. Mauro. SUNNY: a lazy portfolio approach for constraint solving. *Theory and Practice of Logical Programming*, 14(4-5):509–524, 2014.
- Anaconda. The state of data science 2020: Moving from hype toward maturity. *Anaconda*, 2020.
- N. Awad, N. Mallik, and F. Hutter. DEHB: Evolutionary hyperband for scalable, robust and efficient hyperparameter optimization. In Z. Zhou (ed.), *Proceedings of the 30th International Joint Conference on Artificial Intelligence, IJCAI’21*, pp. 2147–2153. ijcai.org, 2021.
- B. Baker, O. Gupta, R. Raskar, and N. Naik. Accelerating neural architecture search using performance prediction. In *International Conference on Learning Representations Workshop track*, 2018. Published online: iclr.cc.
- B. Bischl, P. Kerschke, L. Kotthoff, M. Lindauer, Y. Malitsky, A. Frechette, H. Hoos, F. Hutter, K. Leyton-Brown, K. Tierney, and J. Vanschoren. ASlib: A benchmark library for algorithm selection. *Artificial Intelligence*, 237:41–58, 2016.
- B. Bischl, M. Binder, M. Lang, T. Pielok, J. Richter, S. Coors, J. Thomas, T. Ullmann, M. Becker, A. Boulesteix, D. Deng, and M. Lindauer. Hyperparameter optimization: Foundations, algorithms, best practices and open challenges. *arXiv preprint arXiv:2107.05847*, 2021a.
- B. Bischl, G. Casalicchio, M. Feurer, F. Hutter, M. Lang, R. Mantovani, J. van Rijn, and J. Vanschoren. Openml benchmarking suites. In J. Vanschoren, S. Yeung, and M. Xenochristou (eds.), *Proceedings of the Neural Information Processing Systems Track on Datasets and Benchmarks*. Curran Associates, 2021b.
- M. Blondel, O. Teboul, Q. Berthet, and J. Djolonga. Fast differentiable sorting and ranking. In H. Daume III and A. Singh (eds.), *International Conference on Machine Learning*, volume 98, pp. 950–959. PMLR, Proceedings of Machine Learning Research, 2020.
- O. Bohdal, L. Balles, B. Ermis, C. Archambeau, and G. Zappella. PASHA: efficient HPO with progressive resource allocation. *CoRR*, 2022.
- J. Bossek and H. Trautmann. Multi-objective performance measurement: Alternatives to PAR10 and expected running time. In Y. Hamadi and M. Schoenauer (eds.), *Learning and Intelligent Optimization - 12th International Conference, LION 12, Kalamata, Greece, June 10-15, 2018, Revised Selected Papers*, volume 7219 of *Lecture Notes in Computer Science*, pp. 215–219. Springer, 2018.
- J. Brandt, M. Wever, D. Iliadis, V. Bengs, and E. Hüllermeier. Iterative deepening hyperband. *arXiv preprint arXiv:2302.00511*, 2023.
- L. Breimann. Random forests. *Machine Learning Journal*, 45:5–32, 2001.
- T. Chen and C. Guestrin. Xgboost: A scalable tree boosting system. In B. Krishnapuram, M. Shah, A. Smola, C. Aggarwal, D. Shen, and R. Rastogi (eds.), *Proceedings of the 22nd ACM SIGKDD International Conference on Knowledge Discovery and Data Mining (KDD)*, pp. 785–794. acm, 2016.
- K. Cho, B. Merrienboer, D. Bahdanau, and Y. Bengio. On the properties of neural machine translation: Encoder-decoder approaches. *arXiv preprint arXiv:1409.1259*, 2014.

- 585 H. Coelho, R. Studer, and M. Wooldridge (eds.). *Proceedings of the Nineteenth European Conference on*
 586 *Artificial Intelligence (ECAI'10)*, 2010. IOS Press.
- 587 T. Cunha, C. Soares, and A. de Carvalho. A label ranking approach for selecting rankings of collaborative
 588 filtering algorithms. In H. Haddad, R. Wainwright, and R. Chbeir (eds.), *Proceedings of the 33rd Annual*
 589 *ACM Symposium on Applied Computing, SAC 2018, Pau, France, April 09-13, 2018*, pp. 1393–1395. ACM,
 590 2018.
- 591 J. Devlin, M. Chang, K. Lee, and K. Toutanova. BERT: pre-training of deep bidirectional transformers
 592 for language understanding. In J. Burstein, C. Doran, and T. Solorio (eds.), *Proceedings of the 2019*
 593 *Conference of the North American Chapter of the Association for Computational Linguistics: Human*
 594 *Language Technologies, NAACL-HLT*, pp. 4171–4186. Association for Computational Linguistics, 2019.
- 595 T. Domhan, J. Springenberg, and F. Hutter. Speeding up automatic hyperparameter optimization of deep
 596 neural networks by extrapolation of learning curves. In Q. Yang and M. Wooldridge (eds.), *Proceedings of*
 597 *the 24th International Joint Conference on Artificial Intelligence (IJCAI'15)*, pp. 3460–3468, 2015.
- 598 A. Dosovitskiy, L. Beyer, A. Kolesnikov, D. Weissenborn, X. Zhai, T. Unterthiner, M. Dehghani, M. Minderer,
 599 G. Heigold, S. Gelly, J. Uszkoreit, and N. Houlsby. An image is worth 16x16 words: Transformers for
 600 image recognition at scale. *arXiv preprint arXiv:12010.11929*, 2020.
- 601 S. Falkner, A. Klein, and F. Hutter. BOHB: Robust and efficient hyperparameter optimization at scale.
 602 In J. Dy and A. Krause (eds.), *Proceedings of the 35th International Conference on Machine Learning*
 603 (*ICML'18*), volume 80, pp. 1437–1446. Proceedings of Machine Learning Research, 2018.
- 604 L. Fehring, J. Hanselle, and A. Tornede. Harris: Hybrid ranking and regression forests for algorithm selection.
 605 In F. Ferreira, Q. Lei, E. Triantafillou, J. Vanschoren, and H. Yao (eds.), *NeurIPS 2022 Workshop on*
 606 *Meta-Learning (MetaLearn 2022)*, 2022.
- 607 N. Fusi, R. Sheth, and M. Elibol. Probabilistic Matrix Factorization for Automated Machine Learning. In
 608 S. Bengio, H. Wallach, H. Larochelle, K. Grauman, N. Cesa-Bianchi, and R. Garnett (eds.), *Proceedings of*
 609 *the 31st International Conference on Advances in Neural Information Processing Systems (NeurIPS'18)*,
 610 pp. 3348–3357. Curran Associates, 2018.
- 611 J. Hanselle, A. Tornede, M. Wever, and E. Hüllermeier. Hybrid ranking and regression for algorithm selection.
 612 In U. Schmid, F. Klügl, and D. Wolter (eds.), *Proceedings of the 43rd German Conference on AI (KI'20)*,
 613 volume 12325 of *Lecture Notes in Computer Science*, pp. 59–72. Springer, 2020.
- 614 F. Hutter, L. Kotthoff, and J. Vanschoren (eds.). *Automated Machine Learning: Methods, Systems, Challenges*.
 615 Springer, 2019. Available for free at <http://automl.org/book>.
- 616 J. Petrak J. Fürnkranz. An evaluation of landmarking variants. In L. Raedt and P. Flach (eds.), *ECML/PKDD*
 617 *2001 Workshop on Integrating Aspects of Data Mining, Decision Support and Meta-Learning*, pp. 57–68.
 618 Springer, 2001.
- 619 K. G. Jamieson and A. Talwalkar. Non-stochastic best arm identification and hyperparameter optimization.
 620 In Arthur Gretton and Christian C. Robert (eds.), *Proceedings of the 19th International Conference on*
 621 *Artificial Intelligence and Statistics, AISTATS*, volume 51 of *JMLR Workshop and Conference Proceedings*,
 622 pp. 240–248. JMLR.org, 2016.
- 623 S. Jawed, H. Jomaa, L. Thieme, and J. Grabocka. Multi-task learning curve forecasting across hyperparameter
 624 configurations and datasets. In N. Oliver, F. Pérez-Cruz, S. Kramer, J. Read, and J. Antonio Lozano
 625 (eds.), *Proceedings of the 22th European Conference on Machine Learning and Principles and Practice of*
 626 *Knowledge Discovery in Databases (ECML/PKDD)*, volume 12975 of *Machine Learning and Knowledge*
 627 *Discovery in Databases*, pp. 485–501. ACM, 2021.
- 628 S. Kadioglu, Y. Malitsky, M. Sellmann, and K. Tierney. ISAC - instance-specific algorithm configuration. In
 629 Coelho et al. (2010), pp. 751–756.

- 630 K. Kandasamy, G. Dasarathy, J. Schneider, and B. Póczos. Multi-fidelity bayesian optimisation with
631 continuous approximations. In Precup & Teh (2017).
- 632 Z. Karnin, T. Koren, and O. Somekh. Almost optimal exploration in multi-armed bandits. In S. Dasgupta and
633 D. McAllester (eds.), *Proceedings of the 30th International Conference on Machine Learning (ICML'13)*,
634 pp. 1238–1246. Omnipress, 2013.
- 635 P. Kerschke, H. Hoos, F. Neumann, and H. Trautmann. Automated algorithm selection: Survey and
636 perspectives. *Evolutionary Computation*, 27(1):3–45, 2019.
- 637 D. Kingma and J. Ba. Adam: A method for stochastic optimization. In *Proceedings of the International
638 Conference on Learning Representations (ICLR'15)*, 2015. Published online: iclr.cc.
- 639 A. Klein, S. Falkner, S. Bartels, P. Hennig, and F. Hutter. Fast bayesian hyperparameter optimization on
640 large datasets. In *Electronic Journal of Statistics*, volume 11, pp. 4945–4968, 2017a.
- 641 A. Klein, S. Falkner, J. Springenberg, and F. Hutter. Learning curve prediction with Bayesian neural networks.
642 In *Proceedings of the International Conference on Learning Representations (ICLR'17)*, 2017b. Published
643 online: iclr.cc.
- 644 A. Klein, S. Falkner, J. Springenberg, and F. Hutter. Learning curve prediction with bayesian neural networks.
645 In Precup & Teh (2017).
- 646 R. Leite and P. Brazdil. Predicting relative performance of classifiers from samples. In R. Greiner (ed.),
647 *Proceedings of the 21st International Conference on Machine Learning (ICML'04)*. Omnipress, 2004.
- 648 R. Leite and P. Brazdil. Active testing strategy to predict the best classification algorithm via sampling and
649 metalearning. In Coelho et al. (2010), pp. 309–314.
- 650 L. Li, K. Jamieson, G. DeSalvo, A. Rostamizadeh, and A. Talwalkar. Hyperband: A novel bandit-based
651 approach to hyperparameter optimization. *Journal of Machine Learning Research*, 18(185):1–52, 2018.
- 652 L. Li, K. Jamieson, A. Rostamizadeh, E. Gonina, J. Ben-tzur, M. Hardt, B. Recht, and A. Talwalkar. A
653 system for massively parallel hyperparameter tuning. In *Proceedings of Machine Learning and Systems*,
654 2020.
- 655 M. Lindauer, K. Eggensperger, M. Feurer, A. Biedenkapp, D. Deng, C. Benjamins, T. Ruhkopf, R. Sass, and
656 F. Hutter. SMAC3: A versatile bayesian optimization package for hyperparameter optimization. *Journal
657 of Machine Learning Research (JMLR) – MLOSS*, 23(54):1–9, 2022.
- 658 D. Long, S. Zhang, and Y. Zhang. Performance prediction based on neural architecture features. *Cognitive
659 Computation and Systems*, 2(2):80–83, 2020.
- 660 L. Metz, N. Maheswaranathan, R. Sun, C. Freeman, B. Poole, and J. Sohl-Dickstein. Using a thousand
661 optimization tasks to learn hyperparameter search strategies. *arXiv preprint arXiv:12002.11887*, 2020.
- 662 A. Mohan, T. Ruhkopf, and M. Lindauer. Towards meta-learned algorithm selection using implicit fidelity
663 information. In *ICML 2022 Workshop Adaptive Experimental Design and Active Learning in the Real
664 World (ReALML 2022)*, July 2022.
- 665 F. Mohr and J. van Rijn. Fast and informative model selection using learning curve cross-validation. *arXiv
666 preprint arXiv:12111.13914*, 2021.
- 667 F. Mohr and J. van Rijn. Learning curves for decision making in supervised machine learning - A survey.
668 *CoRR*, abs/2201.12150, 2022.
- 669 F. Mohr, T. Viering, M. Loog, and J. van Rijn. Lcdb 1.0: An extensive learning curves database for
670 classification tasks. In *Machine Learning and Knowledge Discovery in Databases. Research Track -
671 European Conference, ECML PKDD*, 2022.

- 672 M. Nguyen, N. Grinsztajn, I. Guyon, and L. Sun-Hosoya. MetaREVEAL: RL-based Meta-learning from
 673 Learning Curves. In G. Kreml, V. Lemaire, D. Kottke, B. Hammer, and A. Holzinger (eds.), *Workshop*
 674 *on Interactive Adaptive Learning*, 2021.
- 675 V. Nguyen, S. Schulze, and M. Osborne. Bayesian optimization for iterative learning. 2020.
- 676 F. Pedregosa, G. Varoquaux, A. Gramfort, V. Michel, B. Thirion, O. Grisel, M. Blondel, P. Prettenhofer,
 677 R. Weiss, V. Dubourg, J. Vanderplas, A. Passos, D. Cournapeau, M. Brucher, M. Perrot, and E. Duchesnay.
 678 Scikit-learn: Machine learning in Python. *Journal of Machine Learning Research*, 12:2825–2830, 2011.
- 679 B. Pfahringer, H. Bensusan, and C. Giraud-Carrier. Meta-learning by landmarking various learning algo-
 680 rithms. In P. Langley (ed.), *Proceedings of the Seventeenth International Conference on Machine Learning*
 681 (*ICML'00*), pp. 743–750. kaufmann, 2000.
- 682 D. Precup and Y. Teh (eds.). *Proceedings of the 34th International Conference on Machine Learning*
 683 (*ICML'17*), volume 70, 2017. Proceedings of Machine Learning Research.
- 684 D. Pukatov, M. Anastacio, L. Kotthoff, and H. Hoos. Opening the black box: Automated software analysis
 685 for algorithm selection. In I. Guyon, M. Lindauer, M. van der Schaar, F. Hutter, and R. Garnett
 686 (eds.), *Proceedings of the First International Conference on Automated Machine Learning*, volume 188 of
 687 *Proceedings of Machine Learning Research*, pp. 6/1–18. PMLR, 25–27 Jul 2022.
- 688 H. Rakotoarison, L. Milijaona, A. Rasoanaivo, M. Sebag, and M. Schoenauer. Learning meta-features for
 689 autoML. In *Proceedings of the International Conference on Learning Representations (ICLR'22)*, 2021.
 690 Published online: iclr.cc.
- 691 J. Rice. The algorithm selection problem. *Advances in Computers*, 15:65–118, 1976.
- 692 R. Senge, J. José del Coz, and E. Hüllermeier. On the problem of error propagation in classifier chains for
 693 multi-label classification. In M. Spiliopoulou, L. Schmidt-Thieme, and R. Janning (eds.), *Data Analysis,*
 694 *Machine Learning and Knowledge Discovery - Proceedings of the 36th Annual Conference of the Gesellschaft*
 695 *für Klassifikation e. V.*, Studies in Classification, Data Analysis, and Knowledge Organization. Springer,
 696 2012.
- 697 D. Stern, H. Samulowitz, R. Herbrich, T. Graepel, L. Pulina, and A. Tacchella. Collaborative expert portfolio
 698 management. In M. Fox and D. Poole (eds.), *Proceedings of the Twenty-fourth National Conference on*
 699 *Artificial Intelligence (AAAI'10)*. AAAI Press, 2010.
- 700 G. Sui and Y. Yu. Bayesian contextual bandits for hyper parameter optimization. *IEEE Access*, 2020.
- 701 K. Swersky, J. Snoek, and R. Adams. Freeze-thaw bayesian optimization. *arXiv preprint arXiv:11406.3896*,
 702 2014.
- 703 A. Tornede, M. Wever, and E. Hüllermeier. Extreme algorithm selection with dyadic feature representation.
 704 In A. Appice, G. Tsoumakas, Y. Manolopoulos, and S. Matwin (eds.), *Proceedings of the International*
 705 *Conference on Discovery Science (DS)*, pp. 309–324. Springer, 2020.
- 706 J. van Rijn, S. Abdulrahman, P. Brazdil, and J. Vanschoren. Fast algorithm selection using learning curves.
 707 In E. Fromont, T. De Bie, and M. van Leeuwen (eds.), *Proceedings of the 14th International Symposium on*
 708 *Intelligent Data Analysis*. Springer, 2015.
- 709 J. Vanschoren. Meta-learning: A survey. *arXiv preprint arXiv:11810.03548*, 2018.
- 710 J. Vanschoren, J. van Rijn, B. Bischl, and L. Torgo. OpenML: Networked science in machine learning.
 711 *SIGKDD Explorations*, 15(2):49–60, 2014.
- 712 A. Vaswani, N. Shazeer, N. Parmar, J. Uszkoreit, L. Jones, A. Gomez, L. Kaiser, and I. Polosukhin. Attention
 713 is all you need. In I. Guyon, U. von Luxburg, S. Bengio, H. Wallach, R. Fergus, S. Vishwanathan, and
 714 R. Garnett (eds.), *Proceedings of the 30th International Conference on Advances in Neural Information*
 715 *Processing Systems (NeurIPS'17)*. Curran Associates, Inc., 2017.

- 716 M. Wistuba, A. Kadra, and J. Grabocka. Dynamic and efficient gray-box hyperparameter optimization for
717 deep learning. *arXiv preprint arXiv:2202.09774*, 2022.
- 718 L. Xu, F. Hutter, H. Hoos, and K. Leyton-Brown. SATzilla: Portfolio-based algorithm selection for SAT.
719 *Journal of Artificial Intelligence Research*, 32:565–606, 2008.
- 720 L. Xu, F. Hutter, J. Shen, H. Hoos, and K. Leyton-Brown. SATzilla2012: improved algorithm selection
721 based on cost-sensitive classification models. In A. Balint, A. Belov, D. Diepold, S. Gerber, M. Järvisalo,
722 and C. Sinz (eds.), *Proceedings of SAT Challenge 2012: Solver and Benchmark Descriptions*, pp. 57–58.
723 University of Helsinki, 2012.
- 724 L. Zimmer, M. Lindauer, and F. Hutter. Auto-PyTorch Tabular: Multi-Fidelity MetaLearning for Efficient
725 and Robust AutoDL. *IEEE Transactions on Pattern Analysis and Machine Intelligence*, pp. 3079 – 3090,
726 2021.

727 **A Appendix**

728 **A.1 Meta-Datasets**

729 **Synthetic** To demonstrate that MASIF is a non-myopic approach, we create a synthetic function
 730 meta-dataset. A snapshot of the synthetic curve
 731 meta-dataset can be found under Figure 4. To break
 732 the myopic algorithms, we force the curves in one
 733 dataset to intersect at least another curve in an
 734 incrementally way. We initialize by randomly picking
 735 a parametric curve. Subsequent curves are gener-
 736 ated by first sampling a parametric family as de-
 737 scribed by Mohr et al. (2022) and then computing
 738 its parametrization such that it is ensured to inter-
 739 sect with its predecessor. In more detail, we want
 740 to ensure that the intersections occur at different
 741 stages of the training procedure. This is obtained by
 742 randomly selecting one of a few preset intervals in which the intersection is supposed to take place. Repeating
 743 this process for $|\mathcal{A}| - 1$ times produces a single dataset. To make the task more challenging, we add random
 744 noises to the generated curves. To obtain strong meta-knowledge across datasets originating from the shape
 745 of an algorithm's curve, a new dataset is generated by perturbing the parametrization of the existing curves.
 746 Therefore, these datasets contain similar but non-identical curves, that yield variability in the final ranking.
 747 This dataset does not provide dataset meta-features. Overall, we collect 22 datasets each containing 30
 748 learning curves with 51 fidelities.

750 **Task-set** Task-set (Metz et al., 2020) is a meta-dataset that consists of over a thousand tasks ranging from
 751 image classification with fully connected or convolutional neural networks to variational autoencoders on a
 752 variety of datasets. Each task is characterized by 1. an initialization function 2. data split 3. loss function
 753 4. gradients

754 On these tasks, the training, validation, and test curves of multiple optimizer settings have been recorded.
 755 The tasks are additionally organized into families, each pertaining to the kind of problems that they are
 756 trained on. For our experiments, we sub-sampled the tasks from 2 different categories of tasks: Image
 757 Recognition and Language Modeling on text data.

758 The image recognition subset comprises curves generated from fully-connected networks run only on image
 759 recognition tasks, encompassing the following families:

- 760 1. **mlp**: fully-connected networks trained on image data
- 761 2. **mlp_ae**: MLP-based autoencoder trained on image data
- 762 3. **mlp_vae**: MLP-based VAE trained on image data

763 The language modeling subset comprises curves generated from Recurrent Neural Networks (RNNs) trained
 764 on text data, encompassing the following three families:

- 765 1. **char_rnn_language_model**: Language modeling with an RNN on characters.
- 766 2. **word_rnn_language_model**: Language modeling with an RNN on words and subwords.
- 767 3. **rnn_text_classification**: n Text classification using RNN models.

768 We sample the set of algorithms to be the different configurations of the Adam optimizer (Kingma & Ba,
 769 2015) with variations of the learning rate. This allows us to create a meta-dataset of 1000 configurations on

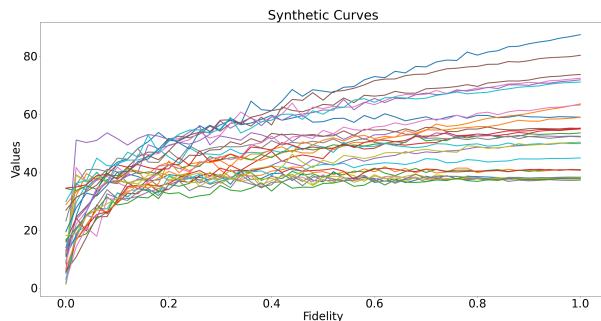


Figure 4: A snapshot of a Synthetic dataset

750 **Task-set** Task-set (Metz et al., 2020) is a meta-dataset that consists of over a thousand tasks ranging from
 751 image classification with fully connected or convolutional neural networks to variational autoencoders on a
 752 variety of datasets. Each task is characterized by 1. an initialization function 2. data split 3. loss function
 753 4. gradients

754 On these tasks, the training, validation, and test curves of multiple optimizer settings have been recorded.
 755 The tasks are additionally organized into families, each pertaining to the kind of problems that they are
 756 trained on. For our experiments, we sub-sampled the tasks from 2 different categories of tasks: Image
 757 Recognition and Language Modeling on text data.

758 The image recognition subset comprises curves generated from fully-connected networks run only on image
 759 recognition tasks, encompassing the following families:

- 760 1. **mlp**: fully-connected networks trained on image data
- 761 2. **mlp_ae**: MLP-based autoencoder trained on image data
- 762 3. **mlp_vae**: MLP-based VAE trained on image data

763 The language modeling subset comprises curves generated from Recurrent Neural Networks (RNNs) trained
 764 on text data, encompassing the following three families:

- 765 1. **char_rnn_language_model**: Language modeling with an RNN on characters.
- 766 2. **word_rnn_language_model**: Language modeling with an RNN on words and subwords.
- 767 3. **rnn_text_classification**: n Text classification using RNN models.

768 We sample the set of algorithms to be the different configurations of the Adam optimizer (Kingma & Ba,
 769 2015) with variations of the learning rate. This allows us to create a meta-dataset of 1000 configurations on

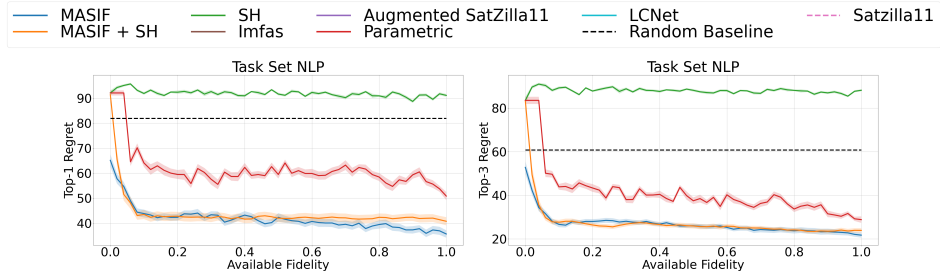


Figure 5: Average test-set top-1 and top-3 regret over ten meta-dataset folds in the slice evaluation protocol for the NLP subset of Task-set. Available fidelity is expressed in the share of the target fidelity’s budget. The standard deviation originates from five repetitions for each fold.

770 100 tasks. This meta-dataset does not provide dataset meta-features. The rationale is that given the noise
 771 and likely crossings of the curves sampled from realistic tasks, the performance on initial fidelities is not
 772 indicative of the final ranks, making it hard for methods like Successive Halving to get a good regret value
 773 without any form of meta-knowledge.

774 **Scikit-CC18** OpenML-CC18 (Bischl et al., 2021b) is a curated classification benchmark featuring 72
 775 carefully selected datasets from OpenML (Vanschoren et al., 2014) with a variety of desirable properties for
 776 a benchmark (see (Bischl et al., 2021b) for details). We generated learning curves on these datasets for 16
 777 classifiers from Scikit-learn (Pedregosa et al., 2011), namely (i) ExtraTreeClassifier (ii) DecisionTreeClassifier
 778 (iii) MLPClassifier (iv) KNeighborsClassifier (v) SGDClassifier (vi) RidgeClassifier (vii) PassiveAggressiveClassifier
 779 (viii) GradientBoostingClassifier (ix) ExtraTreesClassifier (x) BernoulliNB (xi) LinearSVC
 780 (xii) LogisticRegression (xiii) MultinomialNB (xiv) NearestCentroid (xv) Perceptron (xvi) SVC.

781 We collect their learning curves performing the following procedure for every dataset and learner pair: We
 782 performed three-fold cross-validation and for each of these folds again split 20% off of the training data as
 783 validation data. We then trained the classifier on 5%, 10%, . . . , 100% of the training data and evaluated it on
 784 the train, test, and validation data using accuracy as a loss function. As preprocessing, we imputed missing
 785 feature values with the most frequent one in the training data and one-hot encoded categorical features.
 786 Correspondingly, the budgeted resource is the dataset subset size for this meta-dataset. This dataset provides
 787 dataset meta-features.

788 **LCBench** LCBench (Zimmer et al., 2021) is a meta-dataset, that consists of 2000 hyperparameter
 789 configurations of a funnel-shaped neural net on 35 datasets. To meet the AS setup, we choose a subset of
 790 size 170 of these configurations using a top- k ensembling procedure. In particular, this procedure builds the
 791 union of algorithms over the top-10 performing algorithms per dataset across datasets to ensure that each
 792 algorithm was at least somewhat successful on at least one dataset. Presuming, that hyperparameters change
 793 the inductive bias of a model, we conceive for the purpose of our analysis these configurations as independent
 794 algorithms. Notably because of this, the hyperparameter optimization usually resorts to assuming similarity
 795 of performance w.r.t. hyperparameters. By extension, we expect that we can assume some similarity in the
 796 learning behaviors encoded in their learning curves, that MASIF should be able to exploit. This meta-dataset
 797 provides dataset meta-features.

798

799 A.2 Task-set NLP

800 On the NLP task, depicted in Figure 5, we see the overall tendencies of the image subset Task-set, with the
 801 exception that the parametric learning curve baseline is not able to close the performance gap provided full
 802 fidelity.

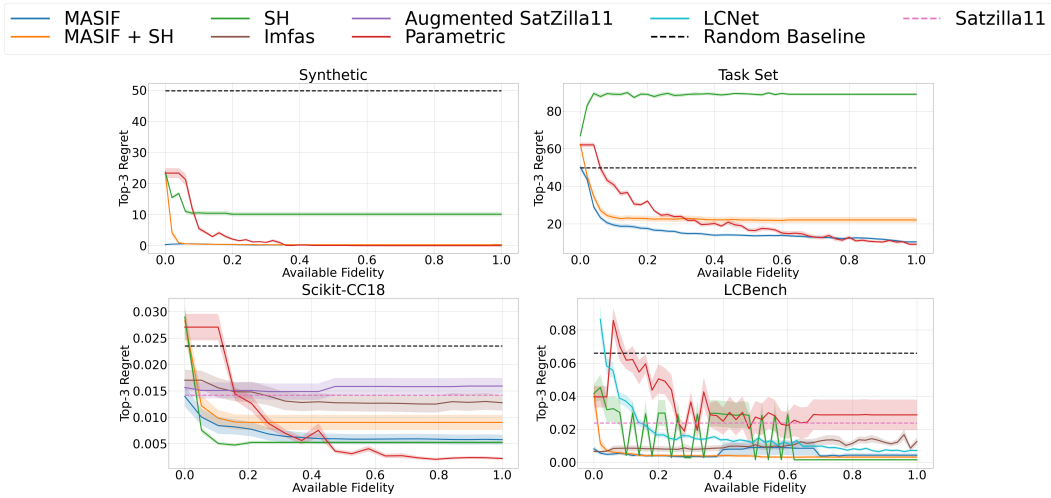


Figure 6: Average test-set top-3 regret over ten meta-dataset folds in the slice evaluation protocol. Available fidelity is expressed in the share of the target fidelity’s budget. The standard deviation originates from five repetitions for each fold. Scikit-CC18 and LCBench exhibit dataset meta-features, while Synthetic and Task-set do not. [Task-set is reported for the image data subset.](#)

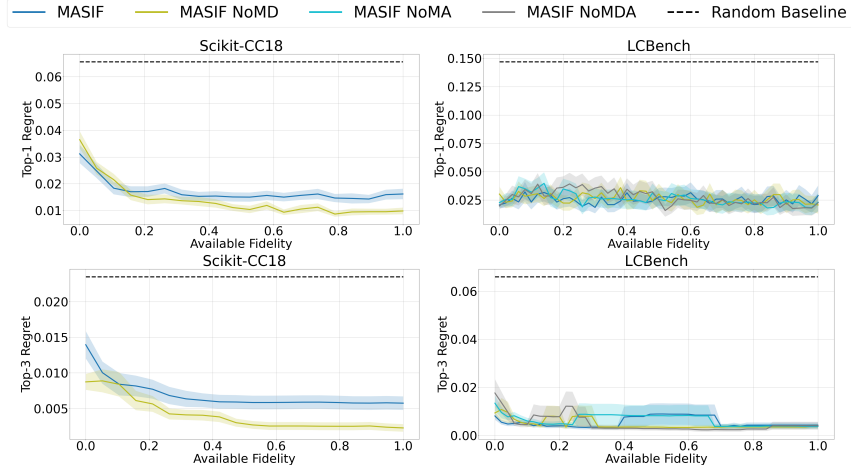


Figure 7: Ablation of MASIF w.r.t. whether or not meta-features are available on Scikit-CC18 (Left) and LCBench (Right) benchmarks. ‘NoM’ indicates that the subsequently detailed meta-feature information is hidden to the model. In particular, ‘D’ stands for dataset meta-features, ‘A’ for algorithm meta-features.

803 A.3 Top-3 results

804 As increasing k in top- k is a hedge, the overall regret is reduced compared to those results of top-1, because it
 805 is more likely to pick the best performer in this enlarged set. The overall tendencies in Figure 6 are however
 806 exactly the same as described in Section 4.4.

807 A.4 Ablations

808 A.4.1 Dataset & Algorithm Meta Features

809 The results in Figure 7 indicate that the regret difference in whether or not the meta-features are present have
 810 – if any – only negligible effect for the Scikit-CC18 and LCBench dataset, once the scale of this difference
 811 is considered. On the other hand, the results in Figure 8 detail, the regret gap, when using a secondary

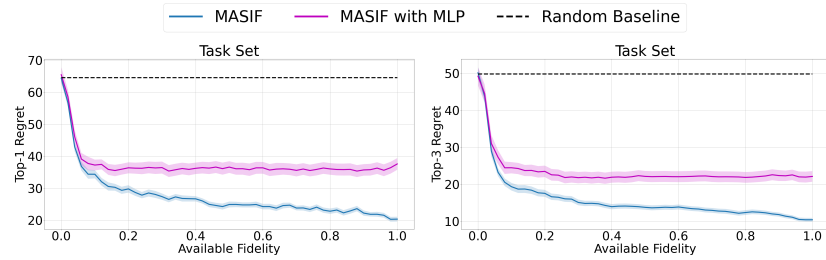


Figure 8: Ablation of MASIF on Task-set benchmark, switching out the second transformer for a simple MLP on the reduced output as joint interpretation module. [Task-set is reported for the image data subset.](#)

812 transformer over the sequence of algorithms rather than an MLP, supporting our design choice for the former.
 813 The vector representation of the learning curves as output to the first transformer holds positional information
 814 since an algorithm is presented always in the same order irrespective of the dataset. The secondary transformer
 815 picks up on this positional information more easily than an MLP.

816 **A.4.2 Parametrization**

817 Provided the scarce data available, we cannot reasonably perform hyperparameter optimization on the
 818 meta-level without risking overfitting. Instead, we consider how the design choices regarding the model's
 819 hyperparameters are affecting performance marginally on Task-set, depicted in Figure 9. As AdamW with
 820 5% linear warm-up and cosine decay is a default choice for optimizing transformers, we added an ablation
 821 to it. Since the number of attention heads, the number of transformer layers affect the model's capability
 822 in describing functions, these hyperparameters are relevant choices. Similarly, dropout should help the
 823 robustness of the transformer. We do, however, find that our model is relatively robust to changes in these
 824 hyperparameters. The overall tendencies and results are the same across hyperparameter configurations. The
 825 slight performance improvements for the marginal alterations prompted us towards trying their combination,
 826 i.e. AdamW with linear warm-up and cosine decay with a learning rate of 0.001, dropout of 0.4 and 4 as
 827 number of transformer layers (as depicted in Figure 9 bottom right). To validate the design choice, we checked
 828 the performance of this promising combination on the remaining benchmarks as depicted in Figure 10 as a
 829 validation set. We do not find the improvements observed on Task-set to consistently yield improvements on
 830 these benchmarks, which is why we are defaulting to the hyperparametrization described in Section 3.4.

831 **A.5 Discussion on Multi-LCNet**

832 As it is conceptually the closest to our model, we will discuss the differences summarized in 5 more thoroughly.
 833 First, their method considers hyperparameters, which allows exploiting the similarities in that space to
 834 interpolate between algorithms - which eases our assumption of a discrete and rigidly observed \mathcal{A} in the
 835 meta-training set and therefore is rather hyperparameter optimization than AS. Second, they leverage
 836 multi-modal data; i.e. multiple auxiliary curves such as e.g. the layer's gradient information are tracked
 837 during training. These curves are only accessible for all configurations, because they limit themselves to a
 838 single class of algorithms, in their case funnel-shaped neural nets. These secondary curves are not necessarily
 839 available for all candidate algorithms considered in an AS model and as such, the method cannot be applied
 840 in our setting. Besides, considering SH's almost oracle performance on LCBench in Figure 3 with a sizeable
 841 subset of 170 algorithm configurations in our experiments, the multi-modal nature of their analysis may not
 842 be a driver for their performance on this particular dataset. Third, their focus is on explicitly extrapolating
 843 single learning curves at a higher fidelity in an auto-regressive manner based on the meta-learned weights of
 844 their Gated Recurrent Units (Cho et al., 2014) that only combine the information from the partial learning
 845 curves of the same algorithm observed from multiple modes of data. Instead, our method leverages the joint
 846 evidence of all invested computations in addition to the meta-knowledge and avoids explicit extrapolation.
 847 Fourth, their handcrafted loss metric is intended to foster good predictions early on, which, despite working
 848 with rather small budgets, might yield suboptimal decisions. Similarly to the SH baseline, this seems to

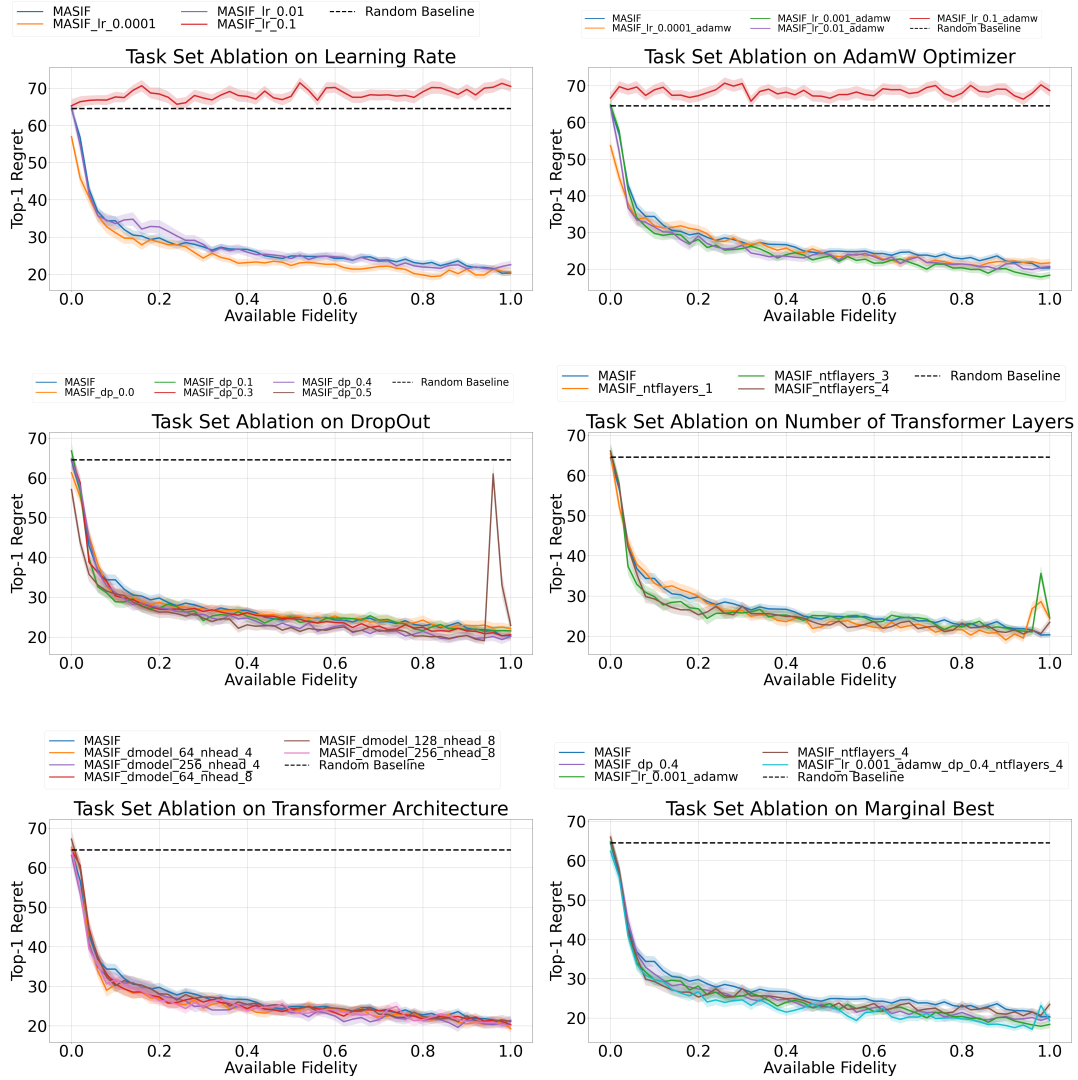


Figure 9: **Ablations of MASIF with marginal changes in the hyperparametrization on Task-set benchmark on all its folds with 5 seeds respectively.** The marginally changed parameters are Adam’s learning rate (lr), the learning rate of AdamW with 5% linear warm-up and cosine decay (lr_adamw), dropout (dp), number of attention heads (n_head), the number of transformer layers (ntlayers) and their hidden dimensions (d_model). Notably, we jointly looked at d_model & n_heads. The default configuration is depicted in blue and amounts to lr=0.001, dp=0.2, n_heads=4, ntlayers=2, d_model=128. Task-set is reported for the image data subset.

849 express and favour a particular budgetary preference over the resulting regret. In contrast, as mentioned
 850 several times, MASIF is much more flexible regarding the budget-regret trade-off.

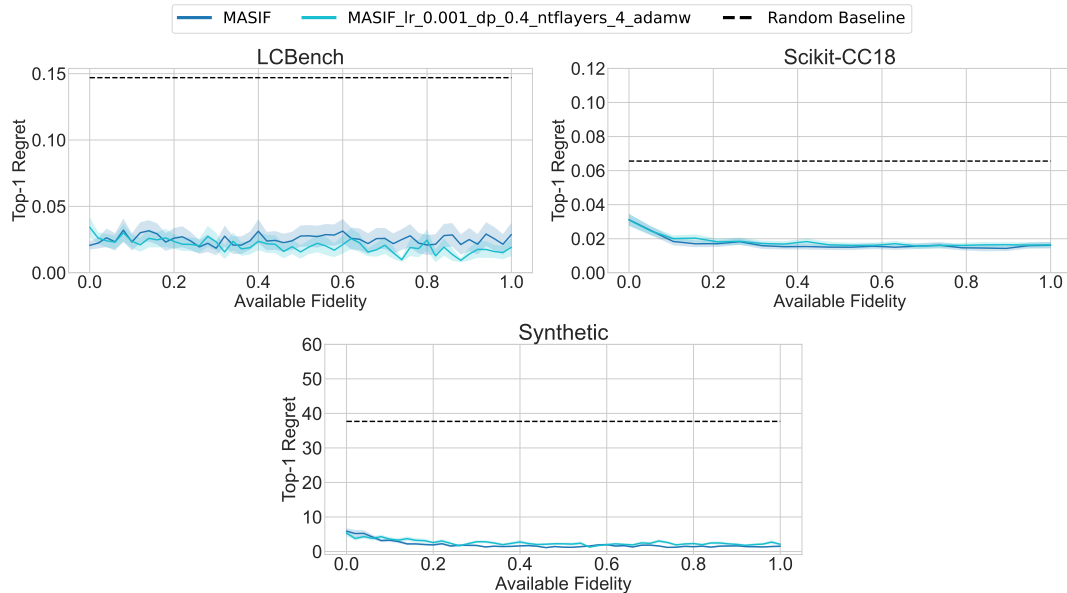


Figure 10: We apply the optimal configuration on the Taskset benchmarks to the other benchmarks. However, the optimal configuration on the Taskset benchmark does not show better performance compared to MASIF’s default setting.

851 **A.6 Reproducibility Statement**

- 852 • Where can the code be found? MASIF’s code is published on [https://anonymous.4open.science/
853 status/MASIF-824D](https://anonymous.4open.science/status/MASIF-824D)
- 854 • What hardware did we use for the experiments? All the experiments are executed on 4 Intel Xeon
855 E5 cores with 8000MB RAM.
- 856 • What hyperparameter settings did we use? How did we get to those? Where can they be found? Using
857 Hydra (hydra.cc) as base package for all our experiment pipelines – including the preprocessing of
858 dataset & algorithm meta-features as well as those for the learning curves, all of the configurations
859 detailing the used models and their configurations can be found in the “configs” folder in the linked
860 repository.
- 861 • What are the requirements in terms of packages and version numbers? The packages & version
862 numbers are available in the setups file of the linked repository.
- 863 • Where can you download our benchmark datasets? We added the newly created Scikit-CC18
864 benchmark as supplementary material. LCBench can be downloaded from [https://github.
865 com/automl/LCBench](https://github.com/automl/LCBench). Task-set can be obtained from [https://github.com/google-research/
866 google-research/tree/master/task_set](https://github.com/google-research/google-research/tree/master/task_set). We provide the Synthetic and Scikit-CC18 benchmarks
867 as supplementary.
- 868 • How many seeds/splits etc. did we perform? We used five seeds and ten folds for each benchmark. A
869 crucial detail regarding the split in the algorithms’ learning curves is described in the dataset section.